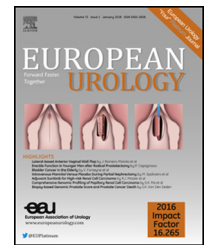


available at www.sciencedirect.com
journal homepage: www.europeanurology.com



European Association of Urology



Prostate Cancer

Patient-derived Hormone-naïve Prostate Cancer Xenograft Models Reveal Growth Factor Receptor Bound Protein 10 as an Androgen Receptor-repressed Gene Driving the Development of Castration-resistant Prostate Cancer

Jun Hao^{a,b,1}, Xinpei Ci^{a,b,1}, Hui Xue^b, Rebecca Wu^b, Xin Dong^b, Stephen Yiu Chuen Choi^{a,b}, Haiqing He^{a,c}, Yu Wang^{a,b}, Fang Zhang^b, Sifeng Qu^{a,b}, Fan Zhang^a, Anne M. Haegert^a, Peter W. Gout^b, Amina Zoubeidi^a, Colin Collins^a, Martin E. Gleave^a, Dong Lin^{a,b,1,*}, Yuzhuo Wang^{a,b,1,*}

^a Vancouver Prostate Centre, Department of Urologic Sciences, Faculty of Medicine, University of British Columbia, Vancouver, BC, Canada; ^b Department of Experimental Therapeutics, BC Cancer Agency, Vancouver, BC, Canada; ^c Department of Urology, The Second Xiangya Hospital, Central South University, Changsha, China

Article info

Article history:

Accepted February 20, 2018

Associate Editor:

James Catto

Keywords:

Androgen deprivation therapy
Castration-resistant prostate cancer
Growth factor receptor bound protein 10
Patient-derived xenografts

Abstract

Background: Although androgen deprivation therapy is initially effective in controlling growth of hormone-naïve prostate cancers (HNPCs) in patients, currently incurable castration-resistant prostate cancer (CRPC) inevitably develops.

Objective: To identify CRPC driver genes that may provide new targets to enhance CRPC therapy.
Design, setting, and participants: Patient-derived xenografts (PDXs) of HNPCs that develop CRPC following host castration were examined for changes in expression of genes at various time points after castration using transcriptome profiling analysis; particular attention was given to pre-CRPC changes in expression indicative of genes acting as potential CRPC drivers.

Outcome measurements and statistical analysis: The functionality of a potential CRPC driver was validated via its knockdown in cultured prostate cancer cells; its clinical relevance was established using data from prostate cancer patient databases.

Results and limitations: Eighty genes were found to be significantly upregulated at the CRPC stage, while seven of them also showed elevated expression prior to CRPC development. Among the latter, growth factor receptor bound protein 10 (*GRB10*) was the most significantly and consistently upregulated gene. Moreover, elevated *GRB10* expression in clinical prostate cancer samples correlated with more aggressive tumor types and poorer patient treatment outcome. *GRB10* knockdown markedly reduced prostate cancer cell proliferation and activity of AKT, a well-established CRPC mediator. A positive correlation between AKT activity and *GRB10* expression was also found in clinical cohorts.

Conclusions: *GRB10* acts as a driver of CRPC and sensitizes androgen receptor pathway inhibitors, and hence *GRB10* targeting provides a novel therapeutic strategy for the disease.

Patient summary: Development of castration-resistant prostate cancer (CRPC) is a major problem in the management of the disease. Using state-of-the-art patient-derived hormone-naïve prostate cancer xenograft models, we found and validated the growth factor receptor bound protein 10 gene as a driver of CRPC, indicating that it may be used as a new molecular target to enhance current CRPC therapy.

© 2018 European Association of Urology. Published by Elsevier B.V. This is an open access article under the CC BY-NC-ND license (<http://creativecommons.org/licenses/by-nc-nd/4.0/>).

¹ These authors contributed equally to this work and should be regarded as joint first and last authors, as appropriate.

* Corresponding authors. Vancouver Prostate Centre, Department of Urologic Sciences, University of British Columbia, 2660 Oak Street, Vancouver, BC, Canada. Tel. +1 604 675 8013; Fax: +1 604 675

<https://doi.org/10.1016/j.eururo.2018.02.019>

0302-2838/© 2018 European Association of Urology. Published by Elsevier B.V. This is an open access article under the CC BY-NC-ND license (<http://creativecommons.org/licenses/by-nc-nd/4.0/>).

Please cite this article in press as: Hao J, et al. Patient-derived Hormone-naïve Prostate Cancer Xenograft Models Reveal Growth Factor Receptor Bound Protein 10 as an Androgen Receptor-repressed Gene Driving the Development of Castration-resistant Prostate Cancer. Eur Urol (2018), <https://doi.org/10.1016/j.eururo.2018.02.019>

1. Introduction

Prostate cancers (PCa's) are largely dependent on androgens for growth and survival [1], and androgen deprivation therapy (ADT) has become the standard treatment for locally advanced or metastatic PCa [2,3]. While most PCa patients initially respond positively to androgen ablation, castration-resistant prostate cancer (CRPC) inevitably develops. Current therapies for CRPC, for example, chemotherapy based on docetaxel or next-generation androgen receptor pathway inhibitors (ARPIs) such as enzalutamide (ENZ) and abiraterone (ABI), can extend patients' lives but are not curative as resistance to their use gradually emerges [4]. As such, there is a critical need for identification of hitherto unrecognized molecular mechanisms that drive the development of CRPC and may lead to novel targets that can be used in combination with ARPIs for more effective therapy.

The present study was aimed at identifying potential CRPC driver genes, in particular genes the elevated expression of which not only initiates but also sustains CRPC. Such genes would have a more important role in the development of CRPC, by inducing bypass pathways circumventing the androgen receptor (AR) pathway, than genes elevated only in CRPC that would mainly be involved in the aggressive growth of CRPCs. We postulated that CRPC driver genes should: (1) be upregulated in CRPC, (2) show elevated expression prior to, and during, the progression from hormone-naïve prostate cancer (HNPC) to CRPC; and (3) be functionally essential for CRPC development. To this end, patient-derived xenograft (PDX) models of HNPC that develop into CRPC following ADT are powerful tools to identify such drivers [5,6]. In our laboratory, using the subrenal capsule (SRC) grafting technique, we have established over 45 transplantable PCa PDX lines (www.livingtumorlab.com) [6]. In this study, we applied host castration on 10 of our HNPC PDX lines. Following castration, seven of these lines developed recurrent CRPC tumors spontaneously. By longitudinally analyzing the gene expression profiles of these PDX lines before castration, at 12 wk following castration, and after CRPC development, we obtained evidence that the *GRB10* gene fulfills the above criteria for a CRPC driver. The human growth factor receptor bound protein 10 (*GRB10*) gene encodes an adaptor protein that modulates coupling of specific signaling pathways to cell surface receptor kinases [7]. Here, we provided evidence that *GRB10* could be a driver of CRPC development and hence a potential therapeutic target for the disease.

2. Patients and methods

2.1. SRC grafting and development of transplantable HNPC lines

Patient HNPC tissues were cut into pieces ($1 \times 3 \times 3 \text{ mm}^3$) and grafted into the SRC site of male nonobese diabetic/severe combined immunodeficient (NOD/SCID) mice supplemented with testosterone as previously described [6]. The host mice were sacrificed in a CO_2 chamber, following growth for 3–6 mo (or earlier if reaching humane ending point). Tumors were then harvested and regrafted into another set of

NOD/SCID mice at the SRC site. At each passage, the xenografts were harvested, measured, and fixed for histopathological analysis. The PDX lines used in this study were summarized in Supplementary Table 1.

The RNA microarray data of the PDX models used in this study can be accessed through Gene Expression Omnibus (GSE41193), and the Living Tumor Laboratory website (<http://www.livingtumorlab.com/>). Detailed information for other materials and methods is provided in the Supplementary material.

3. Results

3.1. Identification of genes as potential drivers of CRPC development: *GRB10*

To elucidate the molecular mechanisms underlying CRPC development, we applied castration to 10 HNPC PDX models developed in our laboratory (Fig. 1A). Castration of mice bearing such tumors leads, within a week, to a marked reduction in tumor volume accompanied by a substantial drop in host serum prostate-specific antigen (PSA) levels (Fig. 1B), that is, an effect mirroring the clinical response of PCa to ADT. Within a few months after castration, seven of these tumor lines, such as the LTL-313B line, gave rise to castration-resistant tumors and increased host serum PSA levels (Fig. 1B). On the histopathological level, we checked the expression of AR, PSA, and Ki67 in LTL-313B samples collected before and at various time points after host castration, and in recurrent tumors. After the 1st week of host castration, AR had diffused to the cytoplasm and PSA and Ki67 expressions had markedly decreased, indicative of reductions in AR transcriptional activity and cell proliferation (Fig. 1C and Supplementary Fig. 1A). After tumor recurrence (about 4 mo later), the scores of these markers had returned to preCx values, showing even higher expressions of AR and PSA (Fig. 1C and Supplementary Fig. 1A).

Among the 10 HNPC PDX lines, seven developed into CRPC after castration (Supplementary Table 1). To identify potential driver genes of CRPC development, we first analyzed gene expression differences using the seven pairs of PDX CRPC models by comparing each CRPC tumor line with its parental HNPC line. Consistently upregulated genes were then ranked based on their statistical significances between pooled HNPC lines and CRPC lines. Eighty genes were identified to be significantly upregulated in CRPC ($p < 0.05$; Fig. 1D and Supplementary Table 4). Next, we checked the expression of these 80 genes from all 10 HNPC PDX lines collected at 12 wk after castration before the appearance of developed CRPC, as indicated by the sustained inhibition of AR signaling suggested by Gene Set Enrichment Analysis (Supplementary Fig. 1B–E and Supplementary Table 2). Of these 80 genes, *GRB10* was the top-ranked gene based on the statistical significance between HNPCs and castrated samples (Fig. 1E and Supplementary Table 4). Thus, these data demonstrate that *GRB10* is not only upregulated in CRPC tumors, but also increased before CRPC fully develops, suggesting that it is a potential early driver of CRPC development (Supplementary Fig. 1F).

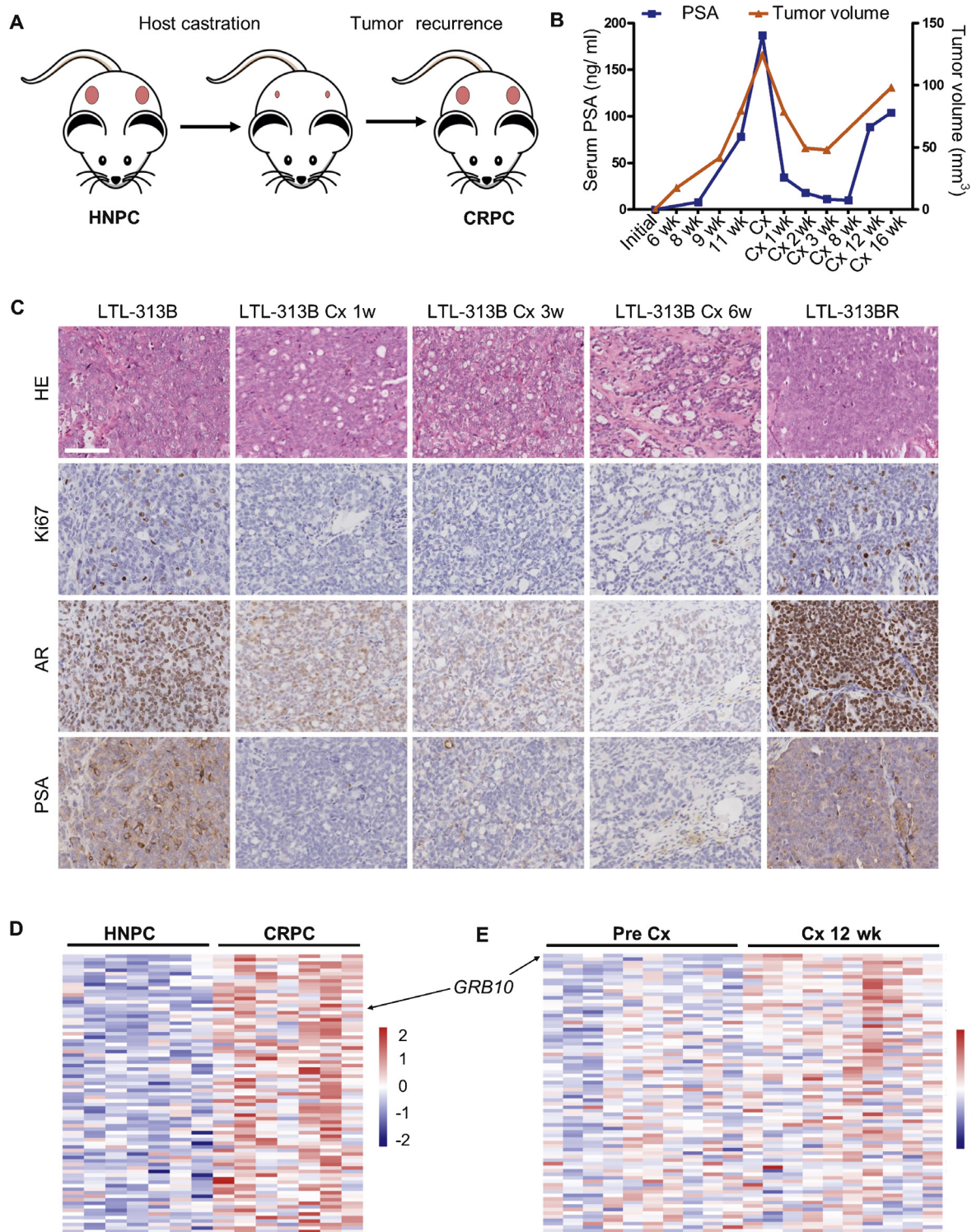


Fig. 1 – Identification of genes as potential drivers of CRPC development: *GRB10*. (A) As illustrated, surgical castration of a mouse bearing subrenal capsule PDXs (pink) of a patient's hormone-naïve prostate cancer (HNPC) led to reduction in tumor volume and, a few months later, to tumor recurrence, that is, CRPC development. (B) Volumes of HNPC LTL-313B xenografts and mouse serum PSA levels at various time points before, during, and after castration-induced CRPC development. (C) Hematoxylin and eosin staining of LTL-313B tumor sections, as well as the levels of Ki67, AR, and PSA in tumor sections (determined via immunohistochemistry) at various time points before and after host castration, and in recurrent tumors. Scale bar indicates 100 μ m. (D) A heat map showing that in seven PDX lines, 80 genes were significantly upregulated in CRPCs compared with their parental HNPCs. (E) A heat map showing *GRB10* as the most consistently upregulated gene of the 80 genes following host castration. Genes ranked according to p value (Student's t-test). A detailed list of genes and gene expression changes used in Figure 1D and E is shown in Supplementary Table 4. AR = androgen receptor; CRPC = castration-resistant prostate cancer; Cx = castration; *GRB10* = growth factor receptor bound protein 10; HE = hematoxylin and eosin; PDX = patient-derived xenograft; PSA = prostate-specific antigen.

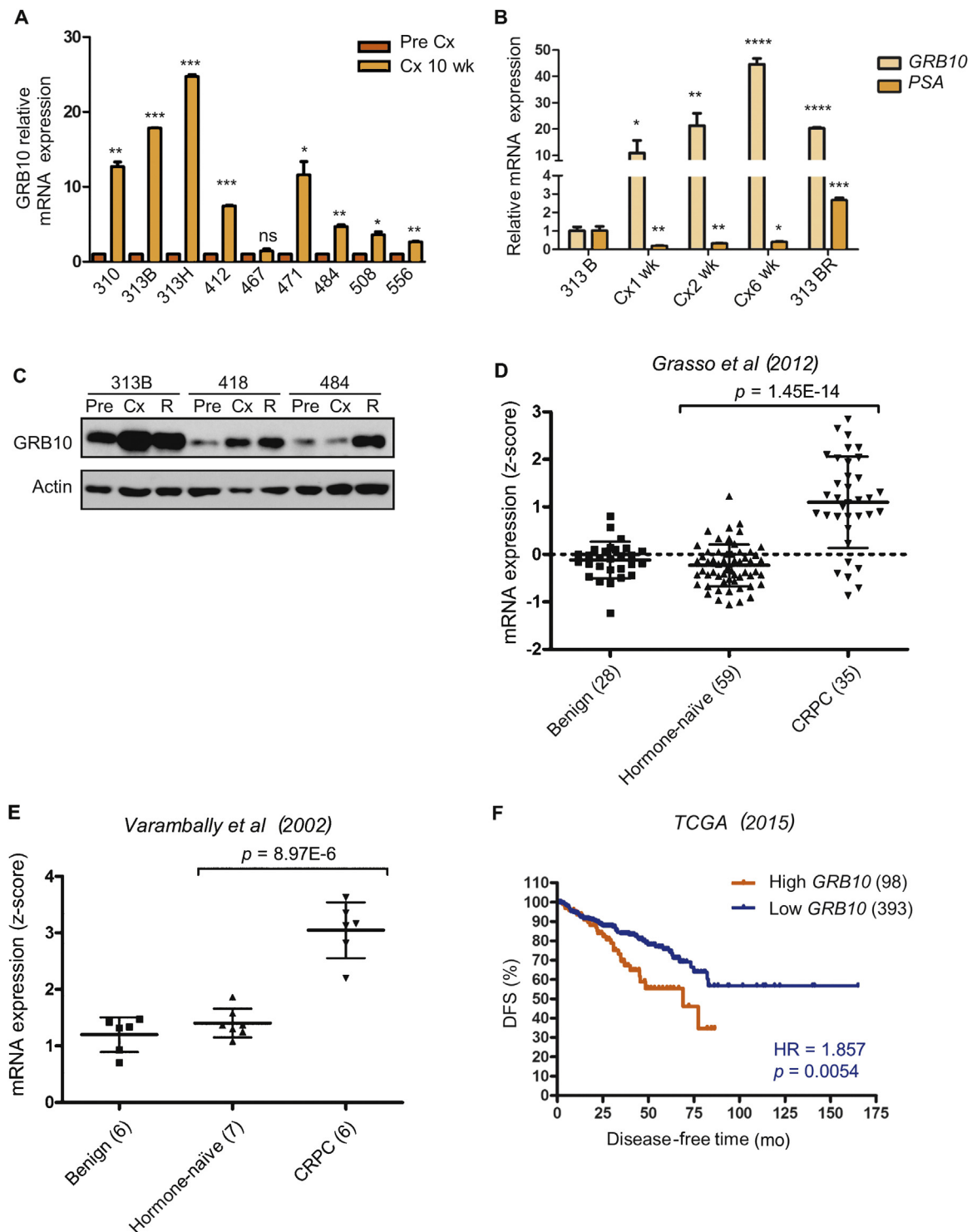


Fig. 2 – Elevated expression of GRB10 in PDX and patient CRPC tissues. (A) Effects of host castration on the expression of *GRB10* in multiple PDX HNPC lines as determined by qRT-PCR; *p* values for each tumor line were determined relative to its parental tumor. The results are presented as means \pm SEM. *p* values for each sample were determined based on paired parental tumors (*: $p < 0.05$; **: $p < 0.01$; ***: $p < 0.001$; ns: not significant). (B) *GRB10* and PSA mRNA expressions in the LTL-313B tumor line were determined by qRT-PCR at various time points after host castration; *p* values for each sample were determined relative to parental tumors. Results are presented as means \pm SEM. *p* values for each sample were determined based on gene expression in LTL-313B samples (*: $p < 0.05$; **: $p < 0.01$; ***: $p < 0.001$; ****: $p < 0.0001$; ns: not significant). (C) *GRB10* protein expressions in LTL-313B, LTL-418, and LTL-484 tumor tissues before castration, 10 wk after castration, and after CRPC development were assessed by Western blotting. (D and E) *GRB10* mRNA expressions of benign prostate tissue, hormone-naïve prostate cancer tissue, and CRPC tissue were derived from Grasso et al [10] and Varambally et al [11] clinical prostate cancer cohorts. The vertical scatter plots show means \pm SEM. (F) Kaplan-Meier plots indicate disease-free survival times of prostate cancer patients grouped according to *GRB10* expression. Significance between the groups was analyzed by the log-rank test. CRPC = castration-resistant prostate cancer; Cx = castration; DFS = disease-free survival; GRB10 = growth factor receptor bound protein 10; HNPC = hormone-naïve prostate cancer; HR = hazard ratio; ns = not significant; PDX = patient-derived xenograft; Pre = pre-castration; PSA = prostate-specific antigen; qRT-PCR = quantitative reverse transcription polymerase chain reaction; R = CRPC; SEM = standard error of the mean; TCGA = The Cancer Genome Atlas; wk = weeks after castration.

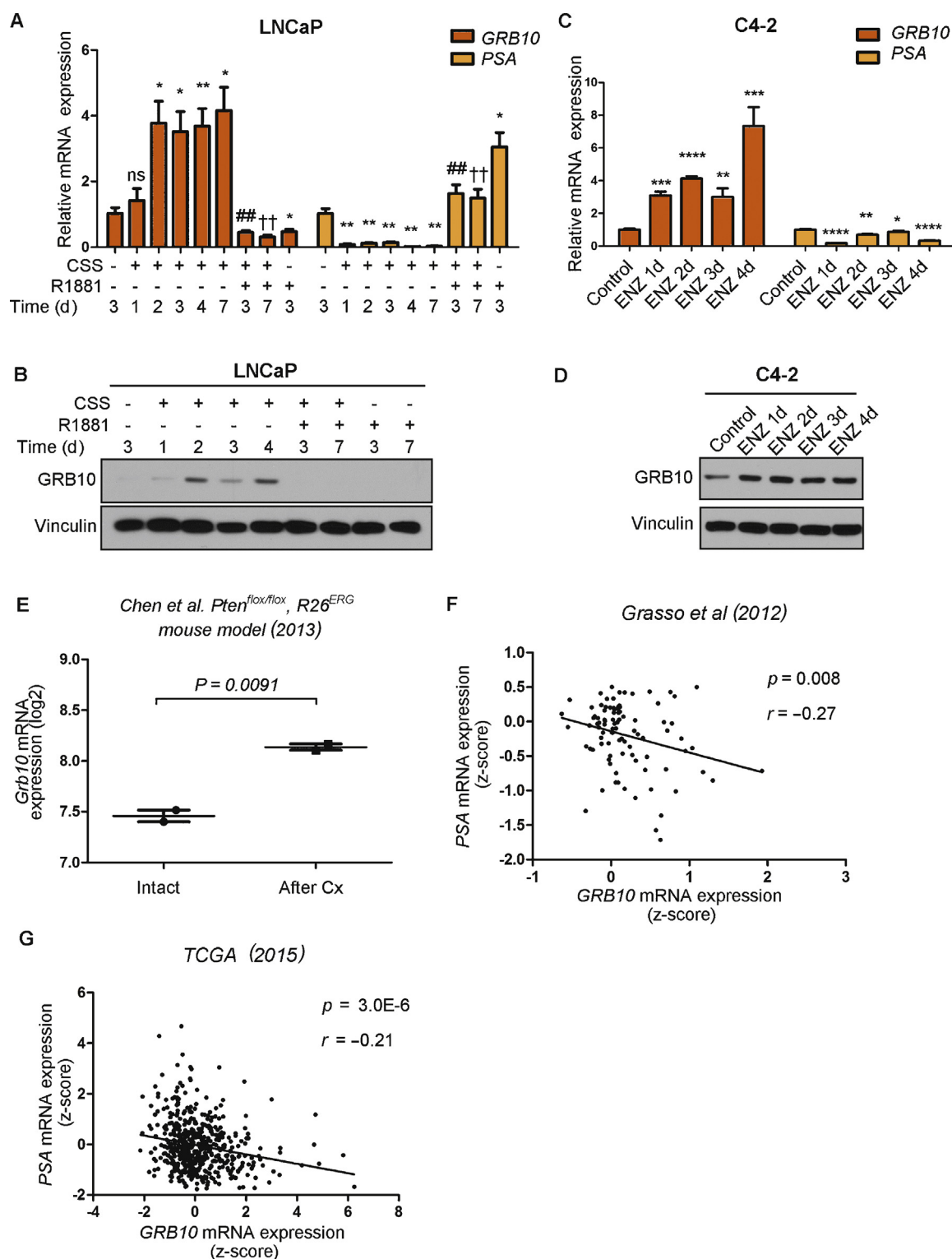


Fig. 3 – GRB10 is an AR-repressed, ADT-inducible-gene in AR⁺ prostate cancer cells. (A and B) Effects of androgen deprivation on GRB10 expression in LNCaP cells (by culturing in CSS medium) were determined by qRT-PCR and Western blotting. To some cultures, 10 nM AR ligand R1881 was added; p values for each sample were determined based on nontreated controls (*), cells cultured in CSS medium for 3 d (#), and cells cultured in CSS medium for 7 d (†) for GRB10 or PSA, respectively. Bar graphs show means \pm SEM. (C and D) Relative GRB10 mRNA and protein expressions in C4-2 cells were determined after treatment with 10 μ M ENZ for various days. Bars show means \pm SEM. (E) *Grb10* mRNA expression in intact and castrated *Pten^{fllox/fllox}, R26^{ERG}* transgenic mouse models constructed by Chenet et al [18]. The vertical scatter plots show means \pm SEM. (F and G) Pearson correlation between GRB10 and PSA mRNA expressions was determined using transcriptomic data of Grasso et al [10] and TCGA [14] clinical prostate cancer cohort. ADT = androgen deprivation therapy; AR = androgen receptor; ENZ = enzalutamide; GRB10 = growth factor receptor bound protein 10; ns = not significant; PSA = prostate-specific antigen; qRT-PCR = quantitative reverse transcription polymerase chain reaction; SEM = standard error of the mean; TCGA = The Cancer Genome Atlas.

3.2. Elevated expression of *GRB10* in PDX and patient CRPC tissues

GRB10 mRNA expression was markedly elevated in post-castration PDX samples (Fig. 2A). As shown in Figure 2B, *GRB10* mRNA levels in the LTL-313B tumor line were markedly elevated following castration, and remained at a high level during CRPC development and at the CRPC stage (ie, in LTL-313BR tumor tissue). Similarly, *GRB10* protein levels were significantly higher in CRPC samples than in the

parental samples (Fig. 2C, and Supplementary Fig. 2D and 2E). *GRB10* was also found to be significantly upregulated in patients' samples collected after neoadjuvant ADT compared with clinical HNPCs in reported clinical cohorts (Supplementary Fig. 2F) [8].

Using publicly available clinical gene expression data [9], we found that the expression of *GRB10* in clinical CRPC samples was significantly elevated compared with hormone-naïve PCa samples [10–12] (Fig. 2D and 2E, and Supplementary Fig. 2G). Additionally, in multiple patient

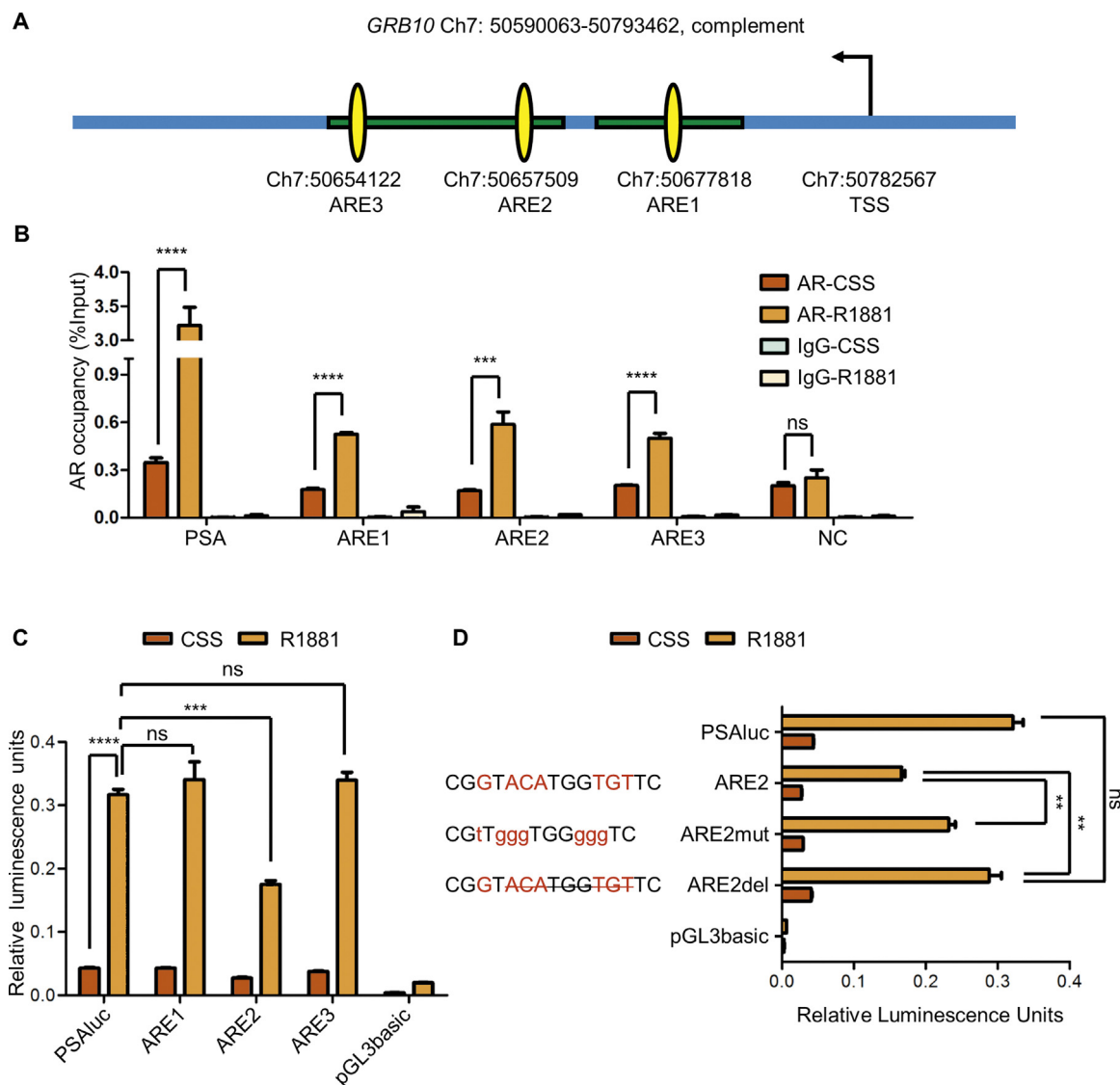


Fig. 4 – AR represses expression of *GRB10* by binding to an ARE located in its intron. (A) Potential androgen-responsive elements (AREs, yellow) and their locations in *GRB10* introns (green) were identified by analysis of reported ChIP-seq data [19]. Based on reported consensus sequences of AREs and use of a computational analysis tool (<http://consite.genereg.net/cgi-bin/consite>), a potential ARE appeared to be located within each of the three potential AR-binding sites. Three potential AREs were labeled based on their distances to the transcription start site (TSS; black arrow). (B) AR occupancies at several DNA locations were measured using ChIP-PCR. The PSA enhancer region (PSA) was used as a positive control, whereas an AR nonbinding site was used as a negative control (NC). Bars show means \pm SEM. (C) Transcriptional inhibitory functions of potential AREs as indicated by reduced luciferase reporter activity. Luminescence units were normalized using Renilla luciferase signal. Bars show means \pm SEM. (D) Transcriptional activation abilities of ARE mutants (sequences are shown) were indicated by dual luciferase reporter assay. Nucleotides in red are sequences of consensus ARE, mutated ARE, and deleted ARE, respectively. Bars show means \pm SEM. ARE = androgen responsive element; Ch7 = chromosome 7; ns = not significant; *GRB10* = growth factor receptor bound protein 10; PCR = polymerase chain reaction; PSA = prostate-specific antigen; SEM = standard error of the mean. p value was calculated (*: $p < 0.05$; **: $p < 0.01$; ***: $p < 0.001$; ****: $p < 0.0001$; ns: not significant).

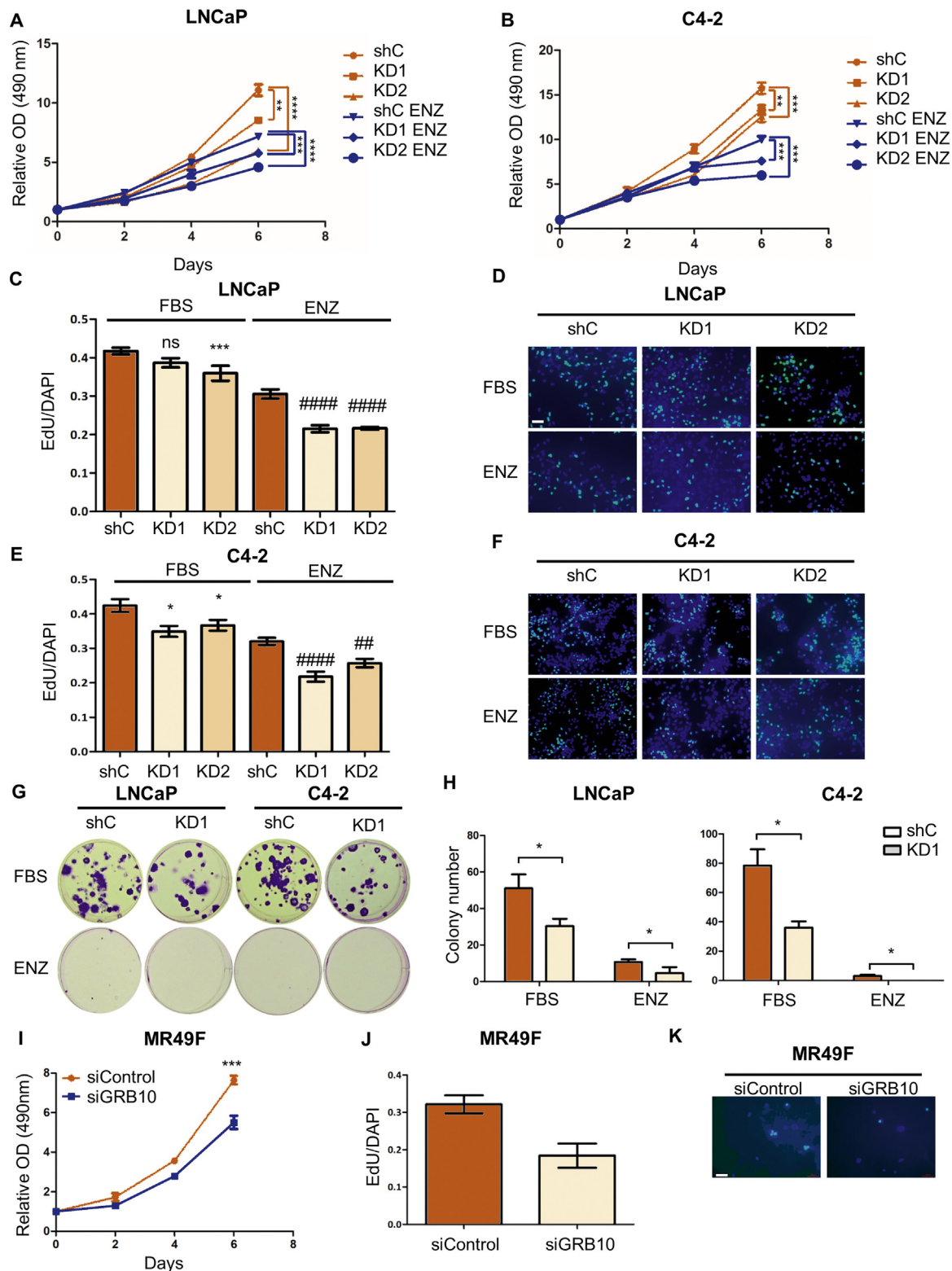


Fig. 5 – *GRB10* knockdown markedly inhibits proliferation, DNA synthesis, and colony formation of prostate cancer cells. (A and B) A potential function of *GRB10* in the proliferation of LNCaP and C4-2 cell lines was determined using stable *GRB10* knockdown (KD1 and KD2) and control (shC) cells and the MTS cell proliferation assay. The effects of treatment of cells with 10 μ M ENZ (in red) was also determined. OD value at 490 nm was normalized based on day 0 readings. Results are presented as means \pm SEM. (C–F) Effects of *GRB10* knockdown on DNA synthesis were determined using an EdU assay; cells were incubated for 4 hours with 10 μ M EdU. EdU-labeled cells (green) and total cell numbers counterstained with DAPI (blue) were counted with 10 images taken at 10-fold magnification. Bars (EdU positive/total cells) show means \pm SEM. Representative images are shown with a 100- μ m scale bar. (G and H) Effects of *GRB10* knockdown on colony formation ability were determined; cells were seeded into six-well plates (100 cells/well) and incubated for 4 wk. Colonies were then stained with crystal violet and imaged; representative images are shown. Bars (colony number of each sample) show means \pm SEM. (I–K) Effects of *GRB10* knockdown on proliferation and DNA synthesis in ENZ-resistant MR49F cells were determined using MTS cell proliferation assay and EdU assay. (I) Transient *GRB10* knockdown (siGRB10) and control (siControl) cells were kept in 10 μ M ENZ containing complete media. OD value at 490 nm

cohorts [12–14], patients exhibiting elevated *GRB10* expression show shorter progression-free survival time (Fig. 2F and Supplementary Fig. 2H–J).

3.3. *GRB10* is an AR-repressed, ADT-inducible gene in AR⁺ PCa cells

To address AR regulation of *GRB10*, we checked its expression in AR⁺ lineage-related human PCa cells LNCaP and C4-2 subjected to androgen deprivation and AR blockade. In androgen-dependent LNCaP cells, ablation of androgen led to increases in both mRNA and protein expressions of *GRB10*; the upregulated expression could be reduced by addition of the synthetic androgen R1881 (Fig. 3A and B, and Supplementary Fig. 3A). These results are consistent with previous reports [15,16] (Supplementary Fig. 3B and 3C). In androgen-independent but AR-signaling active CRPC C4-2 cells, treatment with the AR antagonist ENZ also led to upregulation of *GRB10* expression (Fig. 3C and 3D, and Supplementary Fig. 3D). We also found that transient depletion of AR can upregulate *GRB10* expression (Supplementary Fig. 3E and 3F). All these data indicate that AR itself is a direct repressor of *GRB10* expression [17]. We next checked the expression of *Grb10* in a murine PCa model [18]. *Grb10* was significantly elevated in mice subjected to castration (Fig. 3E). Furthermore, in multiple PCa clinical cohorts [10–14], the expression of *GRB10* in PCa samples tends to be negatively correlated with PSA expression (Fig. 3F and 3G, and Supplementary Fig. 3G–J).

3.4. AR represses expression of *GRB10* by binding to an androgen responsive element located in its intron

To examine whether *GRB10* is transcriptionally regulated by AR, we analyzed chromatin immunoprecipitation sequencing (ChIP-seq) data of AR [19]. Three potential AR-binding sites were identified to be located in the *GRB10*'s intron region, that is, androgen responsive element (ARE)1, ARE2, and ARE3 (Fig. 4A). To confirm the occupancy of AR on these predicted AREs, ChIP-PCR assays were performed on LNCaP cells treated with 10 nM R1881 or ethanol (control). The treatment with R1881 resulted in significant AR enrichment at all three AREs (Fig. 4B). Consistently, similar AR enrichment on the *GRB10* gene was also observed in other AR ChIP-seq data (Supplementary Fig. 4A) [15,20]. Interestingly, the occupancy of AR on the *GRB10* gene was enriched in the samples of untreated PCa patients and decreased in the samples of ADT-responsive patients (Supplementary Fig. 4B) [20]. To further confirm the biological function of AR binding at these potential AREs, we performed a dual luciferase reporter assay. The relative luciferase signals from the reporter plasmid into which ARE2 had been inserted (PSAluc-ARE2) were significantly reduced by treatment

with R1881; this was not found for reporter plasmids containing ARE1 or ARE3 (Fig. 4C). We then constructed two modified PSAluc-ARE2 reporter plasmids in which the consensus sequence of ARE was either mutated or deleted. These modifications led to the rescue of the luciferase signal (Fig. 4D). Taken together, the data demonstrate that AR can act as a transcriptional repressor of *GRB10* by binding to an ARE located in the *GRB10* intron region.

3.5. *GRB10* knockdown markedly inhibits proliferation, DNA synthesis, and colony formation of PCa cells

Following the observation of *GRB10* expression and its upregulation upon ARPI in LNCaP and C4-2 cells (Supplementary Fig. 5A and Fig. 3A–D), we subsequently utilized these two cell lines to determine its cellular function. Stable knockdown of *GRB10* led to marked inhibition of LNCaP and C4-2 cell proliferation (Fig. 5A and B, and Supplementary Fig. 5B and 5C). Combining *GRB10* knockdown and treatment with ENZ led to increased inhibition of cell proliferation (Fig. 5A and B). Knockdown of *GRB10* regardless of ENZ treatment led to decreased DNA synthesis and delayed cell cycle progression (Fig. 5C–F and Supplementary Fig. 5D, 5E, 7D, and 7E). Moreover, knockdown of *GRB10* restricted colony formation by the cells, especially when combined with ENZ treatment (Fig. 5G and H). Furthermore, transient depletion of *GRB10* led to a significant inhibition of cell proliferation and cell cycle progression in the ENZ-resistant PCa cell line MR49F [21] (Fig. 5I–K and Supplementary Fig. 5F and 5G). To determine the function of *GRB10* in driving ARPI resistance, we overexpressed *GRB10* in LNCaP cells and treated them with ENZ. Notably, *GRB10* overexpression partially led to ENZ resistance (Supplementary Fig. 5H, 5I, and 7F). Together, these results suggest that *GRB10* is a driver of CRPC development, and *GRB10*-targeting therapy could enhance the antitumor ability of ARPI and suppress the development of CRPC.

3.6. *GRB10* knockdown reduces AKT activity in PCa cells

AKT is a well-established driver of CRPC [22]. As reported for other systems, *GRB10* can enhance or reduce activity of AKT [7]. Here, we observed that knockdown of *GRB10* in LNCaP, C4-2, and ENZ-resistant MR49F cells consistently led to a decrease in the S473 phosphorylation levels of AKT. Similar results were also observed when the cells were treated with ENZ (Fig. 6A and Supplementary Fig. 5G, 6A, and 6B). The data suggest that *GRB10* promotes AKT activation.

To determine whether *GRB10* can bind to AKT in PCa cells, a co-immunoprecipitation (Co-IP) assay was performed. *GRB10* was able to precipitate AKT, indicating binding of *GRB10* to AKT (Fig. 6B). An immunofluorescence (IF) assay further indicated that endogenous *GRB10* (green)

was normalized based on day 0 readings. Results are presented as means \pm SEM. (J and K) MR49F cells were incubated for 4 h with 10 μ M EdU. EdU-labeled cells (green) and total cell numbers counterstained with DAPI (blue) were counted in 10 images taken at 10-fold magnification. Bars (EdU positive/total cells) show means \pm SEM. Representative images are shown with a 100- μ m scale bar. DAPI = 4',6-diamidino-2-phenylindole; EdU = ethynyl deoxyuridine; ENZ = enzalutamide; FBS = fetal bovine serum; *GRB10* = growth factor receptor bound protein 10; KD1 = *GRB10* stable knockdown cell line 1; KD2 = *GRB10* stable knockdown cell line 2; ns = not significant; OD = optical density; SEM = standard error of the mean; shC = control shRNA stable transfected cells; siControl: MR49F cells transiently transfected with control siRNA; siGRB10 = MR49F cells transiently transfected with *GRB10*-targeting siRNA. *p* value was indicated (*: *p* < 0.05; **: *p* < 0.01; ***: *p* < 0.001; ****: *p* < 0.0001; ns: not significant).

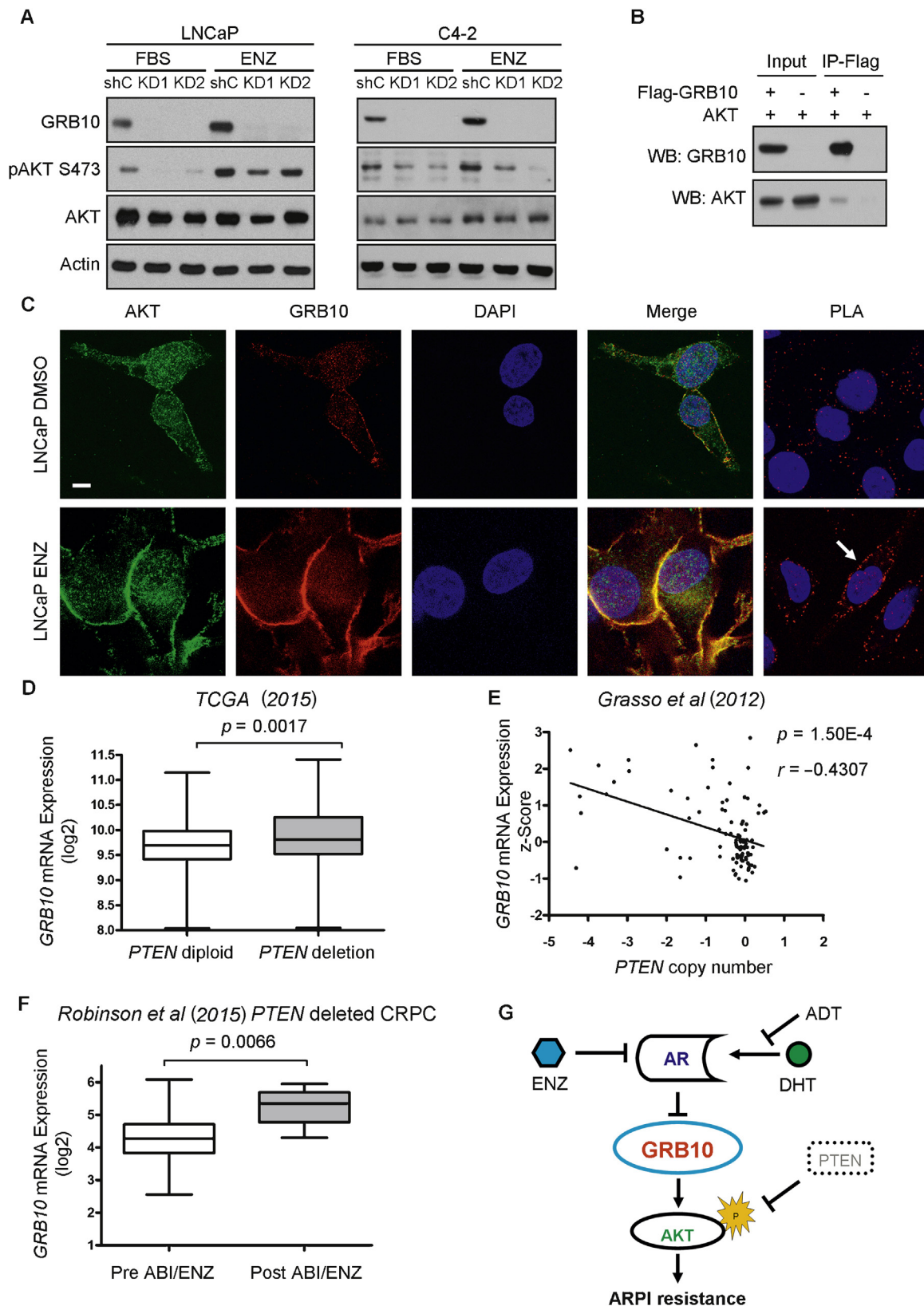


Fig. 6 – GRB10 knockdown reduces AKT activity in prostate cancer cells. (A) Effects of GRB10 knockdown on phosphorylated AKT levels in LNCaP and C4-2 were determined using stable GRB10 knockdown (KD1 and KD2) and control (shC) cell lines, and Western blotting. Total protein was isolated from cells treated with or without 10 μ M ENZ for 3 d. (B) Binding of GRB10 to AKT was confirmed by Co-IP. LNCaP cells expressing Flag-GRB10/AKT or Flag/AKT were collected and lysed with NETN buffer. Five percent of input was collected for each sample. One milligram protein of each sample was incubated with FLAG magnetic beads. Then GRB10 and AKT were detected via Western blotting. (C) AKT (green) and GRB10 (red) localizations in LNCaP cells treated with DMSO (vehicle control) or 10 μ M ENZ were determined using immunofluorescence staining. Representative images are shown with a 10- μ m scale bar. Interaction between AKT and GRB10 was also validated using a proximity ligation assay (PLA). Specific protein-protein interaction

and AKT (red) were colocalized in the cytosol and on the plasma membrane; furthermore, ENZ-treated cells showed more cell membrane colocalizations (Fig. 6C), suggesting that upon ENZ treatment the AKT and GRB10 complex moved toward the plasma membrane where AKT would be activated. In situ interaction between GRB10 and AKT was also indicated by the proximity ligation assay (PLA; Fig. 6C), consistent with IF results, more PLA signals were found on the plasma membrane when cells were treated with ENZ. These data suggest that GRB10 can bind to AKT and lead to its activation.

3.7. *GRB10 expression in clinical PCa samples is significantly correlated with PI3K-AKT signaling pathway activity*

We then further elucidated the association of GRB10 expression and AKT activation in multiple PCa clinical cohorts. In The Cancer Genome Atlas (TCGA) [14] and Grasso et al [10] cohorts, *GRB10* upregulation was significantly correlated with *PTEN* deletion, a well-documented genetic alteration initiating AKT activation in clinical CRPCs (Fig. 6D and E). *GRB10* expression tends to be negatively correlated with *PTEN* expression (Supplementary Fig. 6C–F) [11–13]. Furthermore, *GRB10* expression was found to be significantly upregulated in the *PTEN*-deleted samples following treatment with ABI or ENZ [23] (Fig. 6F), which is consistent with our previous findings. The data support the idea that ADT-induced upregulated expression of *GRB10*, together with *PTEN* deficiency, promotes AKT activation leading to CRPC development (Fig. 6G). As such, *GRB10* may be considered a critical driver of CRPC.

4. Discussion

Development of CRPC is currently the major hurdle in the management of advanced PCa, as next-generation ARPIs such as ENZ and ABI have marginal efficacy [4]. In efforts to develop more effective therapies, it is critical to improve the understanding of the molecular mechanisms underlying the development of CRPC. A major problem of PCa research has been the lack of clinically relevant cancer models and, in particular, models based on patient-derived HNPCs. Unlike other groups using methods involving recombination of patient-derived tissues with mouse seminal vesicle mesenchyme [5], our laboratory has established over 45 transplantable PCa PDX lines, including HNPC, neuroendocrine PCa, and castration-resistant prostate adenocarcinoma, by directly grafting patients' tumor under the mouse renal capsule. Importantly, this technique allows the xenografts to retain key features of the original patients' tumors,

including tumor heterogeneity, tumor microenvironment, tissue architecture, and cancer–stromal interactions. These PDX models also mimic patients' treatment responses, as evident by the observations of spontaneous CRPC development with minimal artificial manipulation [6]. While organoid culturing provides an opportunity to study advanced patient-derived PCa cells in vitro [24], at present, it does not allow the development of HNPC models. Furthermore, although genetically engineered mouse models of PCa are powerful tools for studying mechanisms underlying CRPC development [25,26], they do not reflect the intertumoral genomic heterogeneity of the disease [10,14,23]. In this study, we were able, using seven pairs of hormone-naïve PDX models and related castration-induced CRPC models, to identify common molecular events occurring in CRPC development regardless of a specific genetic background.

AR is well accepted to be responsible for the progression of CRPC [4]. Multiple potent ARPIs have been shown to extend the survival of CRPC patients [27]. However, treatment resistance invariably develops, and in most cases, AR is still promoting cancer progression [4]. Here, we have identified an AR repressed gene, *GRB10*, which is induced by ARPI including androgen ablation and AR blockade, and is highly expressed in CRPC tumors with active AR signaling. In addition, our study showed that *GRB10* is critical for AR⁺ PCa cell proliferation. In AR[−] PCa cell lines such as PC-3 and DU145, where AR expressions are diminished due to other mechanisms [28], the expression of *GRB10* is much lower compared with AR⁺ ones (Supplementary Fig. 5A), indicating other mechanism leading to treatment resistance in those scenarios. Thus, *GRB10* can be considered a universal ARPI resistance-driving gene.

GRB10 has been shown to regulate AKT activation but with contradictory observations in different contexts [7]. For example, *GRB10* has been reported to disrupt the interaction between insulin receptor and insulin receptor substrate 1 in mouse embryonic fibroblasts, eventually leading to inhibition of insulin-induced AKT activation [29]. However, in human leukemic cell lines Mo7e and K562, *GRB10* has been reported to enhance AKT activation independently of PI3-K activity [30,31]. Our finding in the present study clarifies that *GRB10* promotes AKT activation in PCa. Interestingly, we also found that elevated expression of *GRB10* co-occurs with *PTEN* deletion. Consistently, higher endogenous expression of *GRB10* was found in *PTEN*-deleted AR⁺ PCa cell lines (Supplementary Fig. 5A). This evidence suggests that *PTEN* deletion could initiate the baseline expression of *GRB10* together with AKT activation. AKT pathways have been reported to be critical for CRPC

signals are shown in red. (D) A difference in *GRB10* mRNA expression between *PTEN* diploid and *PTEN*-deleted clinical samples was indicated by box-and-whisker plots. Gene expression data were collected from the TCGA [14] patient cohort. (E) A Pearson correlation between *GRB10* mRNA expression and *PTEN* copy number was established. Data were extracted from the Grasso et al [10] patient cohort; the trend line is shown in red. Copy number 0 indicated *PTEN* diploid status. Negative copy number indicated *PTEN* deletion. (F) A difference in *GRB10* mRNA expression between *PTEN*-deleted CRPC patients treated with and without ABI/ENZ was indicated using box-and-whisker plots. Gene expression data were collected from the Robinson et al [23] patient cohort. (G) A schematic model summarizes the mechanisms by which increased expression of *GRB10* by ARPI (ADT/AR signaling inhibitor) mediates ARPI resistance through enhancing AKT activation. ABI = abiraterone; ADT = androgen deprivation therapy; AR = androgen receptor; ARPI = androgen receptor pathway inhibitor; DAPI = 4',6-diamidino-2-phenylindole; DHT = dihydrotestosterone; DMSO = dimethyl sulfoxide; ENZ = enzalutamide; FBS = fetal bovine serum; GRB10 = growth factor receptor bound protein 10; IP = immunoprecipitation; TCGA = The Cancer Genome Atlas; WB = Western blotting.

development and progression [22]. When ARPI is applied, the dramatic upregulation of GRB10 further enhances the activation of AKT, providing proliferative and survival advantages to the residual tumor cells, and ultimately resulting in the development of ARPI resistance. This mechanism could potentially explain the enrichment of *PTEN* deletion in CRPC patients [10,12,13]. However, treatment of CRPC based on targeting only the AKT pathway has had a limited effect [32,33]. As such, targeting GRB10, a potential upstream mediator of AKT, could improve current treatment of CRPC.

With regard to crosstalk between AR and AKT, it has been shown that ADT can lead to increased AKT activity in PCa cells [22]. In this connection, *FKBP5*, an AR-responsive gene, has been reported to promote dephosphorylation of AKT in PCa through recruiting PHLPP phosphatase [34], which leads to the increased AKT activation during ADT. Many studies have shown that AR is highly expressed and transcriptionally active in CRPC [4], suggesting that decreased activity of AKT in CRPC can be expected as a result of recurrent expression of *FKBP5*. However, following the development of CRPC, AKT is still highly active [22], and a better understanding of the crosstalk is required to explain this discrepancy. In the present study, the findings that GRB10 is transcriptionally repressed by AR and mediates the activation of AKT can be used to fill the gap between AR and AKT. Following castration, the expression of GRB10 is elevated, resulting in the activation of AKT. When CRPC has developed, the effect of AR on enhancer elements is stimulated by low castrate levels of androgen, but its effect on suppressor elements remains inhibited [35], leading to consistent upregulation of GRB10 and promotion of AKT activation. This notion is supported by our observations that treatments with ENZ and ABI will further increase GRB10 expression in CRPC. Therefore, our findings provide a molecular bridge between AKT and AR, suggestive of a critical role for GRB10 in the development of CRPC.

5. Conclusions

Using HNPC PDX models and spontaneously developed CRPC, we have shown, for the first time, that GRB10 is a CRPC driver, suggesting a novel therapeutic target to enhance the antitumor ability of current ARPI and delay the development of treatment resistance.

Author contributions: Yuzhuo Wang had full access to all the data in the study and takes responsibility for the integrity of the data and the accuracy of the data analysis.

Study concept and design: Hao, Ci, Lin, Y.Z. Wang.

Acquisition of data: Hao, Ci, Dong, He, Y. Wang, Qu.

Analysis and interpretation of data: Hao, Ci, Choi, Haegert.

Drafting of the manuscript: Hao, Ci, Choi, Gout.

Critical revision of the manuscript for important intellectual content: Hao, Ci, Gout, Zoubeidi, Lin, Gleave, Collins, Y.Z. Wang.

Statistical analysis: Hao, Ci.

Obtaining funding: Collins, Gleave, Y.Z. Wang.

Administrative, technical, or material support: Xue, Wu, Fan Zhang, Fang Zhang, Zoubeidi.

Supervision: Lin, Y.Z. Wang.

Other: None.

Financial disclosures: Yuzhuo Wang certifies that all conflicts of interest, including specific financial interests and relationships and affiliations relevant to the subject matter or materials discussed in the manuscript (eg, employment/affiliation, grants or funding, consultancies, honoraria, stock ownership or options, expert testimony, royalties, or patents filed, received, or pending), are the following: None.

Funding/Support and role of the sponsor: This study was supported by Canadian Institutes of Health Research, Terry Fox Research Institute, BC Cancer Foundation, Urology Foundation, Prostate Cancer Canada, Mitacs Accelerate, Prostate Cancer Canada-Movember, and China Scholarship Council.

Acknowledgments: We would like to thank all members of Y.Z. Wang Laboratory for technical support and helpful discussions. The authors acknowledge Dr. Ladan Fazli for providing anti-PSA and anti-Ki67 antibodies for IHC assay, Dr. Jin-Tang Dong (Emory University, USA) for providing the PSA luciferase reporter plasmid and pSG5-AR plasmid, and Alireza Moeen for IHC image scanning.

Appendix A. Supplementary data

Supplementary data associated with this article can be found, in the online version, at <https://doi.org/10.1016/j.eururo.2018.02.019>.

References

- [1] Jenster G. The role of the androgen receptor in the development and progression of prostate cancer. *Semin Oncol* 1999;26:407–21.
- [2] Huggins C, Stevens RE, Hodges CV. Studies on prostate cancer II The effects of castration on advanced carcinoma of the prostate gland. *Arch Surg* 1941;43:209–23.
- [3] Sharifi N, Gulley JL, Dahut WL. Androgen deprivation therapy for prostate cancer. *JAMA* 2005;294:238–44.
- [4] Yuan X, Cai C, Chen S, Chen S, Yu Z, Balk SP. Androgen receptor functions in castration-resistant prostate cancer and mechanisms of resistance to new agents targeting the androgen axis. *Oncogene* 2014;33:2815–25.
- [5] Lawrence MG, Taylor RA, Toivanen R, et al. A preclinical xenograft model of prostate cancer using human tumors. *Nat Protoc* 2013;8:836–48.
- [6] Lin D, Wyatt AW, Xue H, et al. High fidelity patient-derived xenografts for accelerating prostate cancer discovery and drug development. *Cancer Res* 2014;74:1272–83.
- [7] Riedel H. Grb10 exceeding the boundaries of a common signaling adapter. *Front Biosci* 2004;9:603–18.
- [8] Shaw GL, Whitaker H, Corcoran M, et al. The early effects of rapid androgen deprivation on human prostate cancer. *Eur Urol* 2016;70:214–8.
- [9] Dunning MJ, Vowler SL, Lalonde E, et al. Mining human prostate cancer datasets: the “camcAPP” shiny app. *EBioMedicine* 2017;17:5–6.
- [10] Grasso CS, Wu YM, Robinson DR, et al. The mutational landscape of lethal castration-resistant prostate cancer. *Nature* 2012;487:239–43.
- [11] Varambally S, Dhanasekaran SM, Zhou M, et al. The polycomb group protein EZH2 is involved in progression of prostate cancer. *Nature* 2002;419:624–9.
- [12] Ross-Adams H, Lamb AD, Dunning MJ, et al. Integration of copy number and transcriptomics provides risk stratification in prostate

- cancer: a discovery and validation cohort study. *EBioMedicine* 2015;2:1133–44.
- [13] Taylor BS, Schultz N, Hieronymus H, et al. Integrative genomic profiling of human prostate cancer. *Cancer Cell* 2010;18:11–22.
- [14] Cancer Genome Atlas Research Network. The molecular taxonomy of primary prostate cancer. *Cell* 2015;163:1011–25.
- [15] Massie CE, Lynch A, Ramos-Montoya A, et al. The androgen receptor fuels prostate cancer by regulating central metabolism and biosynthesis. *EMBO J* 2011;30:2719–33.
- [16] Wang Q, Li W, Liu XS, et al. A hierarchical network of transcription factors governs androgen receptor-dependent prostate cancer growth. *Mol Cell* 2007;27:380–92.
- [17] Zegarra-Moro OL, Schmidt LJ, Huang H, Tindall DJ. Disruption of androgen receptor function inhibits proliferation of androgen-refractory prostate cancer cells. *Cancer Res* 2002;62:1008–13.
- [18] Chen Y, Chi P, Rockowitz S, et al. ETS factors reprogram the androgen receptor cistrome and prime prostate tumorigenesis in response to PTEN loss. *Nat Med* 2013;19:1023–9.
- [19] Jin HJ, Zhao JC, Wu L, Kim J, Yu J. Cooperativity and equilibrium with FOXA1 define the androgen receptor transcriptional program. *Nat Commun* 2014;5:3972.
- [20] Sharma NL, Massie CE, Ramos-Montoya A, et al. The androgen receptor induces a distinct transcriptional program in castration-resistant prostate cancer in man. *Cancer Cell* 2013;23:35–47.
- [21] Yamamoto Y, Loriot Y, Beraldi E, et al. Generation 2.5 antisense oligonucleotides targeting the androgen receptor and its splice variants suppress enzalutamide-resistant prostate cancer cell growth. *Clin Cancer Res* 2015;21:1675–87.
- [22] Bitting RL, Armstrong AJ. Targeting the PI3K/Akt/mTOR pathway in castration-resistant prostate cancer. *Endocr Relat Cancer* 2013;20:R83–99.
- [23] Robinson D, Van Allen EM, Wu YM, et al. Integrative clinical genomics of advanced prostate cancer. *Cell* 2015;161:1215–28.
- [24] Gao D, Vela I, Sboner A, et al. Organoid cultures derived from patients with advanced prostate cancer. *Cell* 2014;159:176–87.
- [25] Ellwood-Yen K, Graeber TG, Wongvipat J, et al. Myc-driven murine prostate cancer shares molecular features with human prostate tumors. *Cancer Cell* 2003;4:223–38.
- [26] Wang S, Gao J, Lei Q, et al. Prostate-specific deletion of the murine Pten tumor suppressor gene leads to metastatic prostate cancer. *Cancer Cell* 2003;4:209–21.
- [27] Tombal B, van Soest RJ. Prostate cancer: STAMPEDE, LATITUDE and Fernand Labrie's legacy. *Nat Rev Urol* 2017;14:588–90.
- [28] Jarrard DF, Kinoshita H, Shi Y, et al. Methylation of the androgen receptor promoter CpG island is associated with loss of androgen receptor expression in prostate cancer cells. *Cancer Res* 1998;58:5310–4.
- [29] Yu Y, Yoon SO, Poulgiannis G, et al. Phosphoproteomic analysis identifies Grb10 as an mTORC1 substrate that negatively regulates insulin signaling. *Science* 2011;332:1322–6.
- [30] Jahn T, Seipel P, Urschel S, Peschel C, Duyster J. Role for the adaptor protein Grb10 in the activation of Akt. *Mol Cell Biol* 2002;22:979–91.
- [31] Urschel S, Bassermann F, Bai RY, Munch S, Peschel C, Duyster J. Phosphorylation of grb10 regulates its interaction with 14-3-3. *J Biol Chem* 2005;280:16987–93.
- [32] Chee KG, Longmate J, Quinn DI, et al. The AKT inhibitor perifosine in biochemically recurrent prostate cancer: a phase II California/Pittsburgh cancer consortium trial. *Clin Genitourin Cancer* 2007;5:433–7.
- [33] Posadas EM, Gulley J, Arlen PM, et al. A phase II study of perifosine in androgen independent prostate cancer. *Cancer Biol Ther* 2005;4:1133–7.
- [34] Carver BS, Chapinski C, Wongvipat J, et al. Reciprocal feedback regulation of PI3K and androgen receptor signaling in PTEN-deficient prostate cancer. *Cancer Cell* 2011;19:575–86.
- [35] Cai C, He HH, Chen S, et al. Androgen receptor gene expression in prostate cancer is directly suppressed by the androgen receptor through recruitment of lysine-specific demethylase 1. *Cancer Cell* 2011;20:457–71.